

Comparative Study of the Synthesis and Properties of Vanadate-Exchanged Layered Double Hydroxides

Maria-Angeles Ulibarri

Departamento de Química Inorgánica e Ingeniería Química, Universidad de Córdoba, Facultad de Ciencias, Córdoba 14004, Spain

Francisco M. Labajos, Vicente Rives,* and Raquel Trujillano

Departamento de Química Inorgánica, Universidad de Salamanca, Facultad de Farmacia, Salamanca 37007, Spain

Winnie Kagunya and William Jones

Department of Chemistry, University of Cambridge, Lensfield Road, Cambridge CB2 1EW, U.K.

Received September 1, 1993*

The synthesis and characterization of polyoxovanadate-intercalated MgAl hydrotalcite-like layered double hydroxides (LDH) is described. Seven different methods have been used to intercalate the vanadate anion. These include exchange of the initial carbonate or terephthalate anions, as well as reconstruction of the layered structure from the carbonate form previously calcined at 550 °C—the reconstruction being either directly to the vanadate or indirectly via a terephthalate intermediate. Preswelling with glycerol was also used in some cases. Characterization has been carried out by elemental chemical analysis, powder X-ray diffraction, differential thermal and thermogravimetric analyses, Fourier-transform infrared spectroscopy, transmission electron microscopy, and specific surface area and porosity assessment by nitrogen adsorption at -196 °C. In all cases a layered material containing the $[V_{10}O_{28}]^{6-}$ anion in the interlayer is formed. Direct reconstruction from calcined MgAl LDH with vanadate at pH = 4.5 leads, in addition, to a fibrous material and partial dissolution of magnesium. Experimental results indicate total $CO_3^{2-}/C_6H_4(COO)_2^{2-}$ exchange as well as the absence of glycerol in those cases where it had been used as a preswelling agent. The principal difference between the samples is found within the pore size distribution—a narrow distribution is present in samples prepared via a terephthalate intermediate, while for others the pore size distribution is broader.

Introduction

Layered double hydroxides (LDHs) are a class of layered materials of current interest because of their application in pharmaceutical science and use as adsorbents, catalysts, and anion scavengers. Particularly promising is their application in heterogeneous catalysis, where numerous examples have emerged. A review describing their synthesis, properties, and applications in the above areas as well as others has been recently published.¹

LDHs consist of positively charged brucite-like layers, where partial substitution of M(II) cations by M(III) has occurred; anions are, as a result, incorporated between the layers to balance the resulting excess positive charge. Water molecules also exist in the interlayer space. Hydrotalcite, a naturally occurring LDH, has the formula $Mg_6Al_2(OH)_{16}(CO_3)_4 \cdot 4H_2O$, although when considered as derived from brucite, i.e. $Mg(OH)_2$, this formula may be rewritten as $[Mg_{0.75}Al_{0.25}(OH)_2](CO_3)_{0.125} \cdot 0.5H_2O$.

It is recognized, furthermore, that it would be of considerable value if pillared derivatives of LDHs could be prepared. A variety of procedures have, therefore, been reported concerning the preparation of pillared LDH derivatives.²⁻¹¹ As a result, materials

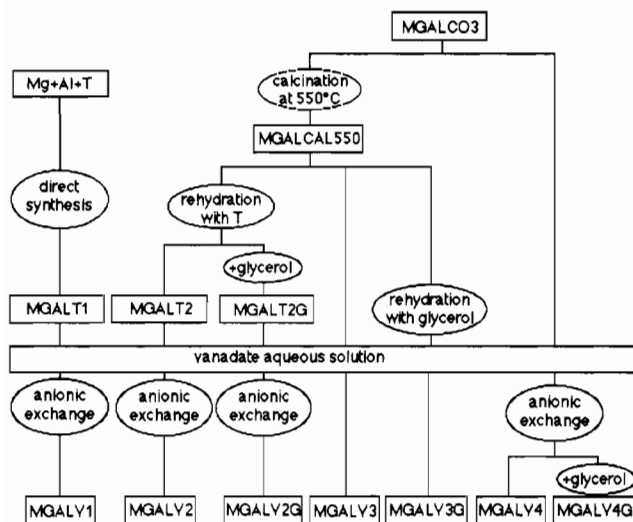
may be prepared with properties akin to those of the well-known pillared clays.¹²

One of the methods for pillaring is based on the fact that calcined LDHs will rehydrate to incorporate guest species. This is an effective route to obtaining a variety of materials² with the method having been applied to intercalate both organic and inorganic anions. Work by Drezdron has shown that the intermediate intercalation of large organic anions assists in the incorporation of inorganic anions, such as iso- and heteropolyoxometalates.³ Such oxoanion pillared materials are of interest as oxidation catalysts (when located in the interlayer space of LDHs, a shape-selective action can be attained¹³) as well as in exhaust gas and hydrocarbon conversion,¹⁴ photooxidation of 2-propanol, and selective oxidation of xylene.^{4,5} Upon thermal decomposition LDHs also result in catalysts which are active for aldol condensation, olefin isomerization, and methanol synthesis via the water-gas shift reaction.¹⁵⁻¹⁹

* Abstract published in *Advance ACS Abstracts*, May 1, 1994.
 (1) Cavani, F.; Trifirò, F.; Vaccari, A. *Catal. Today* **1991**, *11*, 173.
 (2) Chibwe, K.; Jones, W. *J. Chem. Soc., Chem. Commun.* **1989**, 926.
 (3) Drezdron, M. A. *Inorg. Chem.* **1988**, *27*, 4682.
 (4) Kwon, T.; Tsigdinos, G. A.; Pinnavaia, T. J. *J. Am. Chem. Soc.* **1988**, *110*, 3653.
 (5) Twu, J.; Dutta, K. *J. Phys. Chem.* **1989**, *93*, 7863.
 (6) Kwon, T.; Pinnavaia, J. T. *Chem. Mater.* **1989**, *1*, 381.
 (7) Chibwe, K.; Jones, W. *Chem. Mater.* **1989**, *1*, 489.
 (8) Twu, J.; Dutta, P. K. *J. Catal.* **1990**, *124*, 503.

(9) Dimotakis, E. D.; Pinnavaia, T. J. *Inorg. Chem.* **1990**, *29*, 2393.
 (10) Narita, E.; Kaviratna, P.; Pinnavaia, T. J. *Chem. Lett.* **1991**, 805.
 (11) Wang, J.; Tiam, Y.; Wang, R.-C.; Clearfield, A. *Chem. Mater.* **1992**, *4*, 1276.
 (12) Pillared Clays. In *Catalysis Today*; Burch, R., Ed.; Elsevier: Amsterdam, 1988; Vol. 2.
 (13) Tatsumi, T.; Yamamoto, K.; Tajima, H.; Tominaga, H. *Chem. Lett.* **1992**, 815.
 (14) Woltermann, G. M. U.S. Patent 4,454,244, 1988.
 (15) Nakatsuka, T.; Kawasaki, H.; Yamashita, S.; Kohjiya, S. *Bull. Chem. Soc. Jpn.* **1979**, *52*, 2449.
 (16) Kelkar, C. P.; Schultz, A.; Marcelin, G. *ACS Symp. Ser.* **1988**, No. 368, 324.
 (17) Reichle, W. T. *J. Catal.* **1985**, *94*, 547.

Scheme 1. Diagram Illustrating the Various Routes Followed for the Synthesis of the Terephthalate and Vanadate Materials



Of particular importance to potential catalytic application is a reproducible control of the microstructure and composition of the catalyst material. To explore some of the variables associated with the preparation of polyoxometallate-pillared LDHs, we have chosen to study the structural characteristics of a range of vanadium-pillared samples which have been prepared by a variety of procedures. Vanadium was chosen for detailed study because of its use in partial oxidation processes and also because it has been shown²⁰ that LDHs may also be synthesized with V within the layers. Magnesium vanadates are used as catalysts for the synthesis of styrene from the oxidative dehydrogenation of ethylbenzene.²¹⁻²³

It is to be expected that different physical and chemical characteristics will result depending on the preparative route which is used. In particular, crystallinity, surface area, porosity, and purity may all vary. Such variables will influence the potential application and catalytic properties of the final material.

To monitor such variations, we have characterized the materials by powder X-ray diffraction, surface area and porosity measurements, differential thermal analysis and thermogravimetry, transmission electron microscopy, and FT-IR spectroscopy.

Experimental Section

Synthesis Details. The various routes explored are summarized in Scheme 1. All starting materials were from Merck (standard laboratory grade).

(i) **Parent LDH. MGALCO₃.** The parent LDH was synthesized by the method established by Reichle.²⁴ A Mg/Al ratio close to 2 was chosen since this was known from other studies to give samples of good crystallinity. A solution containing 0.1 mol of Mg(NO₃)₂·6H₂O and 0.05 mol of Al(NO₃)₃·9H₂O in 70 mL of deionized water was added with vigorous stirring to a solution of 0.35 mol of NaOH and 0.09 mol of Na₂CO₃ (anhydrous) in 100 mL of deionized water. The addition was over a period of 1 h at room temperature at a pH maintained close to 10. The resulting slurry was then crystallized at 65 °C for 18 h followed by cooling and washing several times with deionized water. The material was dried for 18 h at 100 °C. Elemental analysis confirms that the Mg:Al ratio in the LDH is close to 2 (see Results).

- (18) Reichle, W. T.; Kang, S. Y.; Everhardt, D. S. *J. Catal.* **1986**, *101*, 352.
 (19) Busseto, G.; DelPiero, G.; Manara, G.; Trifiro, F.; Vaccari, A. *J. Catal.* **1984**, *85*, 260.
 (20) Rives, V.; Labajos, F. M.; Ullbarri, M. A.; Malet, P. *Inorg. Chem.* **1993**, *32*, 5000.
 (21) Cortes, A.; Seoane, J. L. *J. Catal.* **1974**, *34*, 7.
 (22) Hanuza, J.; Jezowska-Trzebiatowska, B.; Oganowski, W. *J. Mol. Catal.* **1985**, *29*, 169.
 (23) del Arco, M.; Holgado, M. J.; Martin, C.; Rives, V. *J. Mater. Sci. Lett.* **1987**, *6*, 616.
 (24) Reichle, W. T. *Solid State Ionics* **1986**, *22*, 135.

(ii) **Calcined Precursor Oxide. MGALCAL550.** MGALCO₃ was calcined in air at 550 °C for 18 h to give MGALCAL550. The nature of this decomposition has been extensively studied, and it has been demonstrated that provided calcination is below 550 °C reconstruction of the material to an essentially pure LDH is possible.^{2,7,9,25}

(iii) **Terephthalate Intercalates. (a) MGALT1 Direct Synthesis.** A 1-L three-necked round-bottom flask equipped with reflux condenser, thermometer, mechanical stirrer, and electric heating mantle was charged with 320 mL of boiled (to remove oxygen and carbon dioxide) and deionized water, and 26.6 g of terephthalic acid (0.16 mol) and 115 g of 50% NaOH solution (1.44 mol) were added. Nitrogen was passed through the system until the mixture had cooled to room temperature. Air was then carefully excluded. A solution containing 82.02 g of Mg(NO₃)₂·6H₂O and 60.00 g of Al(NO₃)₃·9H₂O in 250 mL of deionized and boiled water was added dropwise, over a period of approximately 4 h, to the vigorously stirred terephthalate/NaOH solution at room temperature. After addition of the nitrate solution, the mixture was maintained at 75 °C overnight. Upon cooling, the product was isolated by filtration and washed with boiled water. The product was partially dried and then stored in 400 mL of boiled water.

(b) **MGALT2 Rehydration of MGALCAL550.** A 0.2-mol amount of terephthalic acid and 0.4 mol of NaOH in 200 mL of boiled water were mixed, with stirring, in a three-necked round-bottom flask equipped with reflux condenser, and nitrogen was passed for 1 h with the temperature maintained between 60 and 70 °C. A 2-g amount of MGALCAL550 was then added and the mixture stirred for 1 h. The pH of the solution stabilized to a value of 10.2. The product was isolated by filtration and washed with hot water and dried under vacuum at room temperature.

(c) **MGALT2G Rehydration of MGALCAL550 in the Presence of Glycerol.** A 1.0-g amount of MGALCAL550 (3 h of calcination) was added to 50 mL of boiled water in a round-bottom three-necked flask, and nitrogen gas passed for 30 min. The closed system was then stirred for 18 h. 100 mL of glycerol was then added and the mixture further stirred for 6 h. A solution containing 0.54 g of terephthalic acid and 0.26 g of NaOH was added and the mixture stirred for 18 h. The product was isolated by filtration and washed with hot water and dried under vacuum at room temperature.

(iv) **Vanadate-Containing Materials. (a) MGALV1 Anion Exchange of MGALT1.** To a 50-g portion of the slurry of MGALT1 was added a suspension consisting of 3 g of NaVO₃ in 20 mL of deionized and boiled water. The mixture was stirred for 15 min, and then 2 N HNO₃ was added slowly with vigorous stirring until the pH of the solution reached 4.5. After 10 min of additional stirring (at pH 4.5) the product was kept between 65 and 70 °C (without stirring) overnight. Upon cooling, the product was filtered out, washed with boiled water, and dried under vacuum at room temperature overnight.

(b) **MGALV2.** A portion of the slurry containing MGALT2 containing 1.5 g of the solid was deoxygenated by bubbling nitrogen, and 20 mL of a solution containing 1.08 g of NaVO₃ was added. The mixture was magnetically stirred during 15 min, and 2 N HNO₃ was added until pH = 4.5. Then the same procedure described above for sample MGALV1 was followed.

(c) **MGALV2G Anion Exchange of MGALT2G in the Presence of Glycerol.** A 1.52-g sample of NaVO₃ was dissolved in 25 mL of water and HNO₃ added until a pH 4.5 was obtained. This solution was added to the water:glycerol suspension of MGALT2G (previously prepared starting from 1 g of MGALCAL550), and a pH of 4.5 was maintained by the addition of 2 N HNO₃ over a period of 1 h. The mixture was then stirred for a further 4 h (final pH 4.8). The reaction was at room temperature throughout. The product was filtered out, washed with boiled water, and dried under vacuum at room temperature overnight.

(d) **MGALV3 Rehydration of MGALCAL550.** A suspension of 3.05 g of NaVO₃ in 100 mL of deionized and boiled water (0.25 M) was degassed with nitrogen at 65 °C for 15 min. HCl (2 N) then added to give a solution at pH 4.5. A 2-g amount of MGALCAL550 was then added and the pH maintained at 4.5 by the addition of 2 N HCl for 1 h. The mixture was stirred for about 2 h at 65 °C. The product was left (without stirring) at 65 °C for a further 3 days. The product was filtered out, washed with hot water, and dried in vacuum at room temperature.

(e) **MGALV3G Rehydration of MGALCAL550 in the Presence of Glycerol.** A 1-g sample of MGAL550 in 50 mL of deionized and boiled water was stirred for 18 h. A 100-mL volume of glycerol was added and

- (25) Jones, W.; Chibwe, M. In *Pillared Layered Structures: Current Trends and Applications*; Mitchell, I. V., Ed.; Elsevier Applied Sciences: London, 1990; p 67.

Table 1. Elemental Data for the Various Samples Synthesized^a

sample	% Mg	% Al	% V	1-x	x	t	Mg/Al	n
MGALCO3	20.7	10.5		0.69	0.31		2.17	0.87
MGALCAL550	n.m.	n.m.						
MGALT1	17.3	8.9		0.70	0.30		2.32	1.06
MGALT2	16.6	8.2		0.69	0.31		2.24	1.07
MGALT2G	22.2	9.3		0.73	0.27		2.64	n.m.
MGALV1	11.6	6.5	22.5	0.66	0.34	0.62	1.98	0.80
MGALV2	11.8	7.1	21.9	0.65	0.35	0.58	1.84	n.m.
MGALV2G	11.8	6.9	21.9	0.66	0.34	0.58	1.90	n.m.
MGALV3	10.1	9.1	21.8	0.55	0.45	0.57	1.23	1.02
MGALV3G	13.3	6.8	26.6	0.68	0.32	0.65	2.17	n.m.
MGALV4	12.2	7.1	27.1	0.66	0.34	0.70	1.91	1.27
MGALV4G	14.2	6.9	25.4	0.70	0.30	0.60	2.27	n.m.

^a Assuming a formula $[\text{Mg}_{1-x}\text{Al}_x(\text{OH})_2](\text{VO}_y)_z \cdot n\text{H}_2\text{O}$ for the V-containing samples. n.m. = not measured.

the mixture stirred for a further 24 h. A solution of 1.52 g of NaVO_3 in water (plus 2 HCl) at pH 4.5 was added and the pH maintained with 2 N HCl for 1 h. The mixture was stirred for a further 2 h. The product was filtered out and dried at room temperature.

(f) **MGALV4 Anion Exchange of MGALCO3.** To a suspension of 0.5 g of MGALCO3 in 50 mL of water was added, with stirring, a solution of 0.45 g of NaVO_3 in 25 mL of water acidified with 2 N HNO_3 to a pH of 4.5. The pH was maintained for 1 h at this value by the addition of further HNO_3 . The stirring was continued for a further period of 4 h. During the reaction N_2 was purged through the system to remove evolved CO_2 . All processes were at room temperature.

(g) **MGALV4G Anion Exchange of MGALCO3 in the Presence of Glycerol.** The procedure used in part f was repeated except that MGALCO3 was added to a mixture of 50 mL of water to which 100 mL of glycerol had been added. The MGALCO3:water:glycerol mixture was then stirred for 20 h prior to addition of the vanadate solution.

Techniques. Elemental chemical analysis for Mg, Al, and V was performed in a Perkin-Elmer Model 3100 atomic absorption spectrometer, and C was determined using a Perkin-Elmer 2400C instrument. Powder X-ray diffraction (PXRD) patterns were recorded using a Philips APD 1700 instrument, with Ni-filtered $\text{Cu K}\alpha$ radiation. Transmission electron micrographs were obtained using a JEOL 2010 microscope operating at 200 kV; samples were prepared by deposition from an acetone suspension onto a holey carbon film. The FT-IR spectra of the solids were recorded in a Perkin-Elmer FT-IR 1730 spectrometer, following the KBr pellet technique; nominal resolution was 2 cm^{-1} , and 50 scans were averaged. Differential thermal analysis (DTA) and thermogravimetric analysis (TG) of the samples were carried out in Perkin-Elmer DTA-1700 and TGS-2 apparatuses, respectively, coupled to a Perkin-Elmer 3600 data station; the heating schedule was $10\text{ }^\circ\text{C}/\text{min}$ in all cases, and nitrogen or dry air (both from Sociedad Castellana del Oxígeno, SCO, Valladolid, Spain) was passed over the sample during the analysis. Specific surface area and porosity assessment was carried out by nitrogen adsorption at $-196\text{ }^\circ\text{C}$ in a conventional high-vacuum system on samples previously outgassed in situ at $200\text{ }^\circ\text{C}$; pressure changes were monitored with a Baratron MKS pressure transducer; analysis of porosity data²⁶ was carried out with the assistance of a computer program.²⁷

Results and Discussion

Samples MGALCO3, MGALCAL550, MGALT1, MGALT2, and MGALT2G are white, while those containing vanadium show the typical yellow–orange color of V_2O_5 and other V^{5+} -containing compounds resulting from $\text{O}^{2-} \rightarrow \text{V}^{5+}$ charge transfer.

Elemental Analysis. Results for chemical analysis of the samples are given in Table 1. As expected, the Mg/Al ratio in the initial sample (MGALCO3) is close to 2, and it does not change significantly in all other samples containing terephthalate or vanadate as the counteranion with the values centered around 2.1 ± 0.2 . The values determined for samples MGALT2G and MGALV3 were, reproducibly, high and low, respectively. It is likely that the variation in the Mg/Al ratio in the different samples may be related to differences in selective dissolution of Mg or Al during the exchange or rehydration processes. Significantly, the

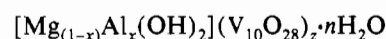
vanadium content also remains reasonably constant for all samples (ca. $23\% \pm 3$) irrespective of the method of preparation.

The carbon content was not analyzed in all samples, due to the similarities previously found for the other elements. C and H were analyzed only in samples MGALT2 (13.8% C, 3.6% H), MGALV4 (0.3 and 2.1%), and MGALV3 (0.3 and 2.1%). The values are consistent with the presence of carbon-containing moieties in the interlayer space of sample MGALT2 but with their absence in those samples containing vanadium, as the content in C is close to the sensitivity of the instrument. These results suggest that carbonate is completely exchanged by vanadate, and when used to aid exchange, glycerol does not itself remain in the interlayer space (see infrared results below).

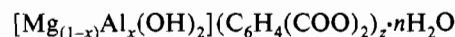
Such analytical data allow a tentative determination of the nuclearity of the vanadium-containing polyoxometalate in the interlayer space. According to the chemical analysis results, it can be assumed that oxovanadate species of the general type $\text{V}_\alpha\text{O}_\beta^{z-}$ are the only counteranions in these samples. As a result, the excess in positive charge in the layers (above the neutrality corresponding to brucite) due to the presence of octahedral substitution Al cations would be balanced by the negative charge of the interlayer counteranion; i.e., the α/γ ratio should balance the aluminum content. From the results included in Table 1, such a ratio is 0.6 for samples MGALV1, MGALV2, and MGALV2G, 0.8 for sample MGALV3, and 0.5 for samples MGALV3G, MGALV4, and MGALV4G. This suggests that in the first set of samples the counteranion is a single species which can be formulated as $[\text{V}_{10}\text{O}_{27.5}]^{5-}$. For the third set of samples the species correspond to $[\text{V}_{10}\text{O}_{28}]^{6-}$ coincident with the ideal value for the pH conditions used. The difference can be reasonably assumed to be within experimental error, and so the interlayer anion would be $[\text{V}_{10}\text{O}_{28}]^{6-}$. However, the value for sample MGALV3 is extremely high, although the behavior shown by this sample is in all cases rather peculiar.

With regards to the results of the C analysis, a similar calculation can be carried out. Thus, sample MGALT2 contains 1.17 mol of C per formula and corresponds to 0.15 mol of terephthalate ($\text{C}_6\text{H}_4(\text{COO})_2^{2-}$) per formula, a value almost coincident with that required to compensate 0.31 mol of Al per formula of compound (0.155).

The chemical analysis results indicate, therefore, that general formulas maybe given as



and



Powder X-ray Diffraction. The powder X-ray patterns for the samples are shown in Figures 1 and 2. The values for the c dimension are given in Table 2. Although these may be calculated as $c = 3d(003)$, the value reported has been calculated from the positions of the (003), (006), and (009) peaks, i.e., $c = [d(003) + 2d(006) + 3d(009)]$, while, for reasons given below, for the vanadium-containing samples it has been calculated from the positions of the (006) and (009) peaks as $c = 3[2d(006) + 3d(009)]/2$.

The pattern for sample MGALCO3, Figure 1a, is characteristic of a LDH with a $c/3$ value of 7.72 \AA , in good agreement with the value of 7.69 \AA reported for an LDH carbonate.¹ This indicates a gallery height of 2.92 \AA (assuming a thickness of 4.8 \AA for the cationic sheets). The material is reasonably crystalline and suggests a relatively well-ordered sheets arrangement, in agreement with previous work²⁸ concerning samples with a Mg:Al ratio close to 2 and the preparation method used. Figure 1b indicates the effect on the X-ray pattern of calcination at $550\text{ }^\circ\text{C}$ in air. The material decomposes to give a semi-amorphous phase with a pattern characteristic of a defect MgO material. The

(26) Shields, J. E.; Lowell, S. *Powder Surface Area and Porosity*, 2nd ed.; Chapman and Hall: London, 1984.

(27) Rives, V. *Adsorpt. Sci. Technol.* **1991**, *8*, 95.



Figure 1. Powder X-ray diffraction patterns for (a) MGALCO₃, (b) MGALCAL550, (c) MGALT1, (d) MGALT2, and (e) MGALT2G.

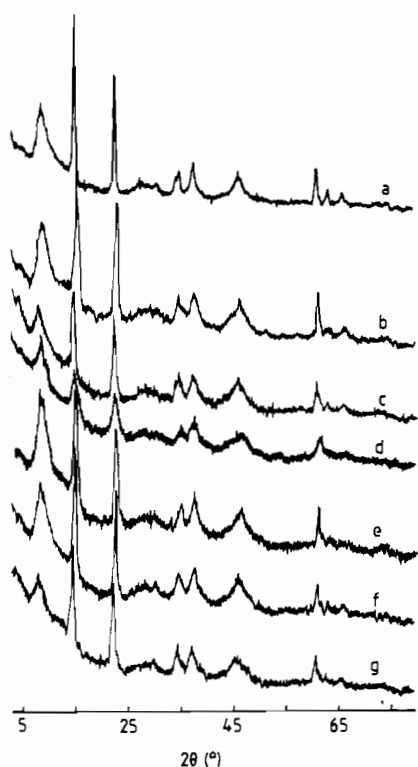


Figure 2. Powder X-ray diffraction patterns for (a) MGALV1, (b) MGALV2, (c) MGALV2G, (d) MGALV3, (e) MGALV3G, (f) MGALV4, and (g) MGALV4G.

most intense peaks of MgO are recorded at 2.09 Å ((200) planes) and 1.48 Å ((220) planes). None of these peaks are observed for samples prepared by reconstruction of MGALCAL550, indicating that no unreacted MgO remains.

The pattern obtained from the terephthalate intercalate prepared by direct synthesis is shown in Figure 1c. The value calculated for c is 43.5 Å, close to the value of 43.2 Å which has been associated with the incorporation of the terephthalate dianion

Table 2. Surface Area and Porosity Data after Calcination at 200 °C

sample	c (Å)	S_{BET} (m ² /g)	sample	c (Å)	S_{BET} (m ² /g)
MGALCO ₃	23.2	77	MGALV2G	31.5	75
MGALT1	44.1	42	MGALV3	31.5	48
MGALT2	43.8	7	MGALV3G	31.9	77
MGALT2G	43.6	8	MGALV4	31.2	89
MGALV1	30.9	56	MGALV4G	32.9	84
MGALV2	29.4	64			

in a vertical arrangement.³ Infrared (see later) confirms that little, if any, of the neutral acid is incorporated. Figure 1d shows the PXRD for MGALT2 which results from exposure of MGALCAL550 to terephthalate solution. The positions of the (003), (006), and (009) peaks yield an average value for c of 43.5 Å, indicating a gallery height of 9.7 Å. The pattern obtained from a sample of MGALT2G, prepared in the presence of glycerol, is shown in Figure 1e. The positions of the reflections are similar ($c/3 = 14.5$ Å) to those above. The use of glycerol does not appear to substantially improve the quality of the pattern, and the gallery height remains unaffected. For all three samples, the position of the (110) reflection remains constant at 1.52 Å, indicating a value of a ($\approx 2d(110)$) of 3.04 Å.

The PXRD patterns for samples containing vanadium species in the interlayer are shown in Figure 2. In each trace, the first peak, close to 10.4 Å, is generally broad. The second and the third peaks, however, are relatively sharp and similar to those recorded for the carbonate- and terephthalate-containing LDHs; see Figure 1. In all cases, the position of the first reflection is incorrect for (003) if the second and third reflections are indexed as (006) and (009), respectively. We interpret this as evidence for a biphasic material—with the reflection at 10.4 Å hiding the (003) reflection of the pillared phases; *vide infra*. The interlayer spacings for vanadium containing samples have therefore been calculated from the positions of the (006) and (009) reflections only.

Figure 2a shows the pattern of MGALV1 resulting from direct anion exchange of MGALT1. It corresponds to intercalated LDH with a gallery height of 7.0 Å, in agreement with that reported by Drezdzone³ for V₁₀O₂₈⁶⁻-intercalated MgAl LDH. There is no evidence for residual carbonate-like material. The pattern in Figure 2b corresponds to MGALV2. The pattern is very similar to that for MGALV1, with a basal spacing of 11.6 Å. Figure 2c shows the pattern obtained when the vanadate exchange occurs in the presence of glycerol, resulting in a basal spacing of 11.8 Å. There is little difference between these three diffractograms.

The X-ray patterns obtained by the incorporation of the vanadate by direct rehydration of MGALCAL550 are also shown in Figure 2d,e. While there is little variation between these two patterns, that for MGALV3 has significantly less well developed (003) and (006) reflections. Finally, Figure 2f,g illustrates the patterns obtained when carbonate in MGALCO₃ is directly exchanged by vanadate, both without and with glycerol, respectively. Again, only minor differences can be distinguished between these two patterns.

The PXRD patterns, therefore, for samples possessing polyoxovanadate in the interlayer space are very similar for all routes. It should be also noted that the a dimension is also constant and coincides with the value calculated for the samples containing carbonate or terephthalate, 3.04 Å. While the gallery height depends on the nature of the counteranion (ca. 7.7 Å for carbonate, 14.5 Å for terephthalate, and 11.8 Å for polyoxovanadate), the value for a in LDHs depends only on the nature of the cations in the layers. The constant value of a obtained in all our samples (3.04 Å) confirms that only Mg²⁺ and Al³⁺ exist in the layer, with no, or little, incorporation of V⁵⁺ into the sheets.

The origin of the broad reflection at ≈ 10.4 Å is, however, unclear. As indicated above, its position is not correct for (003) if the second and third reflections are indexed as (006) and (009).

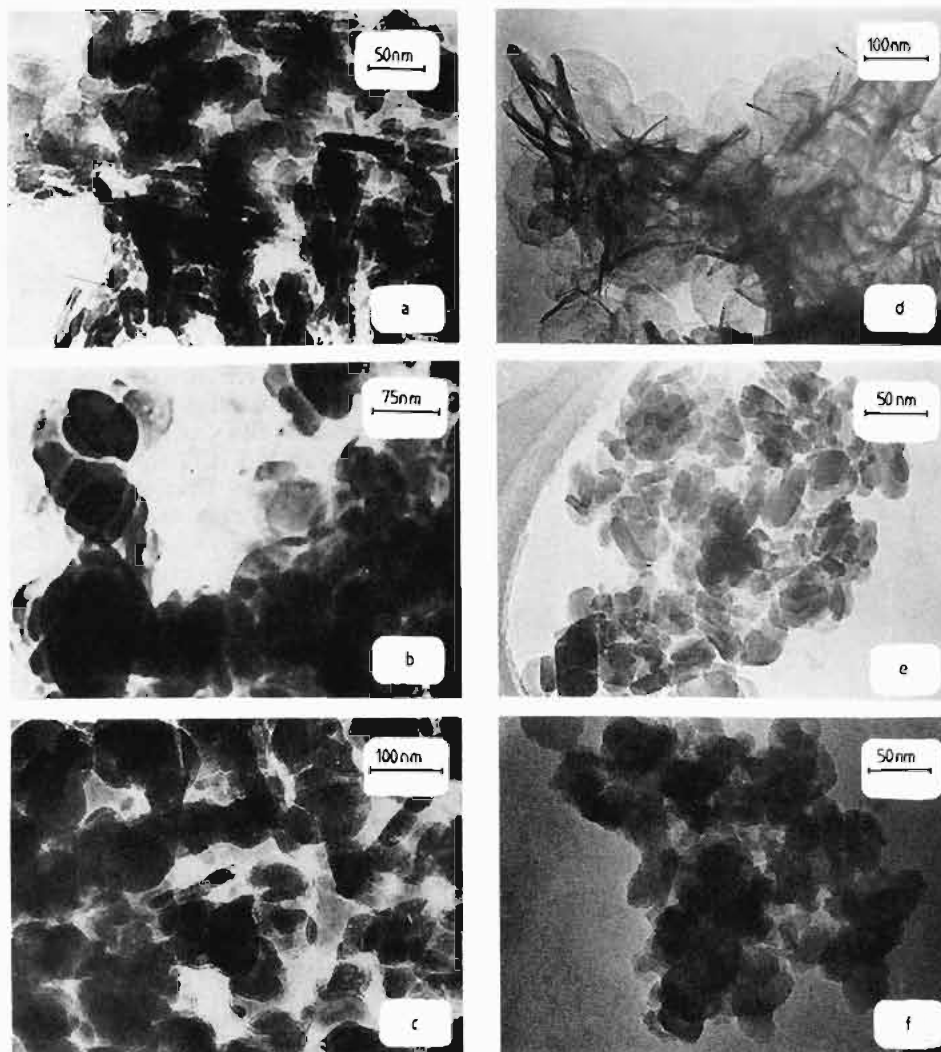


Figure 3. Transmission electron micrographs of (a) MGALCO₃, (b) MGALT1, (c) MGALV1, (d) MGALV3, (e) MGALV3G, and (f) MGALV4.

These are, however, sharp peaks whose position can be determined accurately. From this, the expected position for the (003) peak is always close, but never coincides, with the maximum at ≈ 10.4 Å. A similar broad peak at 10.2–10.9 Å has been also reported by Pinnavaia et al.¹⁰ upon intercalation of $[\alpha\text{-SiW}_{11}\text{O}_{39}]^{8-}$ and $[\alpha\text{-1,2,3-SiV}_3\text{W}_9\text{O}_{40}]^{7-}$ into ZnAl hydrotalcites and has been attributed to Zn²⁺ and Al³⁺ salts of the polyoxometallate (POM). For LDHs intercalated with POM ions possessing the Keggin-type structure, Clearfield et al.¹¹ have reported also a broad PXRD peak at 11–13 Å, which sometimes covers the (003) peak; they ascribe this broad peak to formation of a new compound as a result of the reaction between the basic LDH layers and the acidic POM. Preliminary studies of polyvanadate intercalated Ni₃Al hydrotalcites have shown also a broad PXRD peak at ≈ 11.9 Å, which, depending on the preparation method, can be resolved into a sharp peak at 11.7 Å (fitting well with the expected position for the (003) reflection) and a broader one at 9.8 Å. In this case, TEM-EDAX analysis of the samples indicates two different types of particles, one containing Ni, Al and V and the other without aluminium.

Transmission Electron Microscopy. Transmission electron micrographs of selected samples are shown in Figure 3. Those for samples MGALCO₃, MGALT1, MGALV1, MGALV3G, and MGALV4 (Figure 3a–c, e–f) indicate the existence of lamellar particles with rounded hexagonal shape, typical of hydrotalcite-like materials. However, that for sample MGALV3 (Figure 3d) shows two different types of particles: together with the hexagonal, thin particles, other fibrous particles can be clearly seen. This second type of particles has not been observed in any other sample

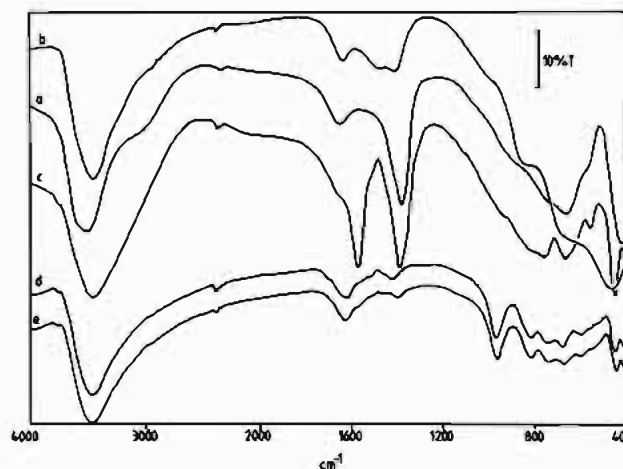


Figure 4. IR spectra obtained for (a) MGALCO₃, (b) MGALCAL550, (c) MGALT1, (d) MGALV2, and (e) MGALV2G.

and confirms the peculiar behavior of this sample, with a low Mg/Al ratio (Table 1) and weak PXRD peaks (see Figure 2).

Infrared Spectroscopy. Figure 4a–e shows the spectra obtained for MGALCO₃, MGALCAL550, MGALT1, MGALV2, and MGALV2G.

The spectrum for sample MGALCO₃, Figure 4a, shows a broad absorption band at 3486 cm⁻¹, with a shoulder at 3575 cm⁻¹. In addition, a second, weaker shoulder is also recorded at ca. 3020 cm⁻¹. These peaks correspond to $\nu(\text{OH})$ stretching modes and have been discussed in detail in a previous paper.²⁸ They are

associated with $\nu(\text{OH})$ of interlayer water, for which the corresponding $\delta(\text{H}_2\text{O})$ peak is recorded at 1653 cm^{-1} , and also to hydroxyl groups of the layers. The presence of hydrogen bonds between hydroxyl groups and water molecules broadens the absorption band. The shoulder slightly above 3000 cm^{-1} has been ascribed^{28–30} to $\nu(\text{OH})$ of water molecules hydrogen bonded to the interlayer carbonate anions. The strong band at 1380 cm^{-1} is due to ν_3 mode of the interlayer carbonate anion. This band is recorded at 1450 cm^{-1} for the free anion,³¹ and the shift observed ($\Delta = 70\text{ cm}^{-1}$) is due to a lower symmetry of this moiety in the interlayer space, probably because of hydrogen bonding with OH groups and/or water molecules. The ordering attained by this sample during preparation has probably favored formation of an ordered structure not only in the layers but also in the interlayer. According to the gallery height calculated from the PXRD results, the carbonate anions lie parallel to the layers and should be hydrogen bonded to several water molecules, thus retaining a D_{3h} symmetry and accounting for a single, nonsplit band due to the ν_3 mode; other bands that would be recorded for lower symmetries (i.e., ν_1 close to 1060 cm^{-1}) are absent in the spectrum. The bands recorded below 800 cm^{-1} are due to lattice vibration mainly involving translational motions and Mg–O, Al–O stretching modes and other bending modes from the layers.

When the solid is calcined at $550\text{ }^\circ\text{C}$, sample MGALCAL550, the most noticeable feature is the loss of the intense band at 1380 cm^{-1} and the shoulder at 3020 cm^{-1} . Both bands are associated with the presence of carbonate ions. The general aspect of the spectrum in the low-wavenumber region (below 800 cm^{-1}) is also different from that for the parent sample.

For the MGALT1 sample, the characteristic doublet formed by two strong bands at 1574 and 1395 cm^{-1} is due to the terephthalate divalent dianion.³² The high-wavenumber band shows also a shoulder at ca. 1635 cm^{-1} , due to the $\delta(\text{H}_2\text{O})$ mode. The $\nu(\text{OH})$ band centered at 3440 cm^{-1} is now broader than in MGALCO₃, probably due to many different hydrogen-bonded hydroxyl groups, with participation of the carboxylate groups of the terephthalate anion. The absence of an absorption close to 1700 cm^{-1} , characteristic of the presence of free acid, confirms that only the anion form is present. On the other hand, the appearance of the spectrum below 800 cm^{-1} is now comparable to that of sample MGALCO₃, corresponding to a real hydroxalite-like material.

The samples containing vanadium show similar spectra, Figure 4d,e. The bands due to terephthalate are absent. The shoulder below 3000 cm^{-1} is also absent, as well as other bands due to the presence of carbonate anions. The bands due to hydroxyl groups and molecular water (ca. 3436 and 1628 cm^{-1}) are present. The most characteristic feature of these two spectra is the medium-intensity band recorded at 977 cm^{-1} . Frederickson and Hausen³³ have shown that crystalline polyvanadates give rise to absorption bands in the 950 – 1000 cm^{-1} region, which have been attributed to the $\text{V}=\text{O}$ terminal stretching mode. The number and exact positions of these bands depends on the number of vanadium ions existing in the polyvanadate. In particular, hexavanadates give rise to two absorption bands in this region, whereas decavanadates give only one band. In our case, one single band at 977 cm^{-1} indicates the presence of decavanadate as the vanadium-containing species. Other bands close to 830 , 751 , 682 , and 600 cm^{-1} coincide with those reported by Lopez-Salinas and Ono for $\text{V}_{10}\text{O}_{28}$ -pillared MgAl LDHs.³⁴

(28) Labajos, F. M.; Rives, V.; Ulibarri, M. A. *J. Mater. Sci.* **1992**, *27*, 1546.

(29) Kruijsink, E. C.; van Reijden, L. L.; Ross, J. R. H. *J. Chem. Soc., Faraday Trans. 1* **1991**, *77*, 649.

(30) Bish, D. L.; Brindley, G. W. *Am. Mineral.* **1977**, *62*, 458.

(31) Nakamoto, K. *Infrared and Raman Spectra of Inorganic and Coordination Compounds*, 4th ed.; Wiley: New York, 1980.

(32) Bellamy, L. J. *The Infrared Spectra of Complex Molecules*, 3rd ed.; Chapman and Hall: London, 1975; Vol. 1.

(33) Frederickson, L. D., Jr.; Hausen, D. M. *Anal. Chem.* **1978**, *23*, 93.

(34) Lopez Salinas, E.; Ono, Y. *Bull. Chem. Soc. Jpn.* **1992**, *65*, 2465.

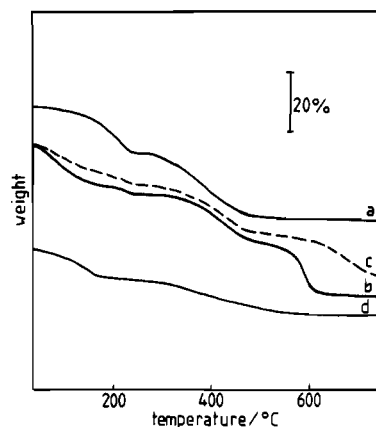


Figure 5. TG curves for (a) MGALCO₃, (b) MGALT1 in air, (c) MGALT1 in nitrogen, and (d) MGALV1.

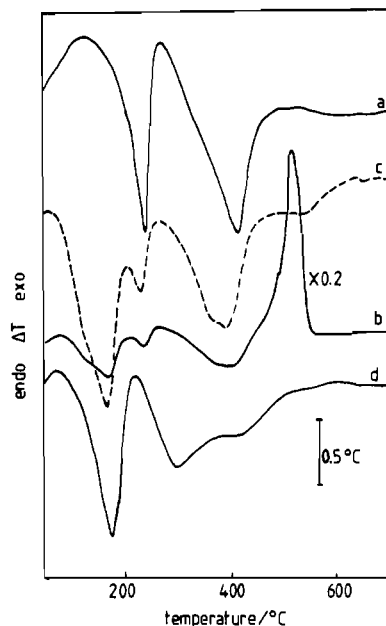


Figure 6. DTA curves for (a) MGALCO₃, (b) MGALT1 in air, (c) MGALT1 in nitrogen, and (d) MGALV1.

Although the broad band close to 3500 cm^{-1} for MGALV3G might be associated with co-intercalated glycerol, the absence of strong absorptions at 1050 cm^{-1} and 1350 – 1260 cm^{-1} (OH deformation and C–O stretching, respectively) indicates that little, if any, glycerol remains in the sample after exchange.

Thermal Analysis. Figure 5 shows the TG for selected samples, while the corresponding DTA profiles are shown in Figure 6. The analyses have been performed in air, although for sample MGALT1 an additional analysis in nitrogen was made, in order to identify those processes associated with combustion. The results are summarized in Table 3. For MGALCO₃, Figure 5a, the losses are in agreement with those reported by others and consist of two steps, the first one up to ca. $280\text{ }^\circ\text{C}$, and represents 18.6% of the initial weight of sample. The second (completely finished at $550\text{ }^\circ\text{C}$) represents a weight loss of 27.4%. In some cases, the second step shows an inflection point, indicating that it is formed by two overlapped processes.^{28,35} Mass spectrometric analysis of the gases evolved during this decomposition has shown³⁶ that the first weight loss corresponds to elimination of water, and the second one to loss of water and CO₂. The temperature ranges where these losses are recorded suggest that the first loss

(35) Pesic, L.; Salipurovic, S.; Markovic, V.; Vucelic, D.; Kagunya, W.; Jones, W. J. *Mater. Chem.* **1992**, *2*, 1069.

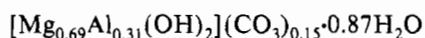
(36) del Arco, M.; Martin, C.; Martin, I.; Rives, V.; Trujillano, R. *Spectrochim. Acta A* **1993**, *49A*, 1575.

Table 3. Thermogravimetric Analysis Results for the Samples Studied

sample	atmosphere	temp range (°C)	% wt loss	<i>n</i> H ₂ O
MGALCO ₃	air	<280	18.6	0.87
		280–740	27.4	
MGALT1	air	<255	18.6	1.06
		255–740	36.2	
	nitrogen	<270	15.6	0.86
MGALT2	air	270–740	32.3	1.07
		<255	18.5	
	nitrogen	255–740	38.2	1.02
MGALV1	air	<255	17.8	1.02
		255–740	37.6	
	nitrogen	<225	10.9	0.80
MGALV3	air	225–740	13.6	1.02
		<225	13.9	
	nitrogen	<225	14.0	1.03
MGALV4	air	225–740	13.2	1.27
		<210	15.4	
	nitrogen	210–740	11.8	

corresponds to elimination of molecular water from the interlayer, while the second involves loss of water from dehydroxylation of the layers. The temperature of 550 °C chosen therefore corresponds to a material for which essentially all the carbonate has been removed and for which significant lattice dehydroxylation has taken place. The weight losses recorded coincide with the two endothermic peaks recorded in the DTA for this sample, with minima at 240 and 415 °C, although the asymmetry of the second peak indicates that it may correspond to two overlapping processes.

The weight loss up to 280 °C can be used to determine the molecular water content (i.e., interlayer water) of the sample. The value calculated corresponds to 0.87 mol of H₂O per brucite-like formula; i.e., the formula of the starting material can be written as



The total weight loss determined experimentally is 48.2%, while the value calculated from the data corresponding to chemical analysis is 46%—the agreement being good, within experimental error.

In the case of MGALT1, Figures 5b,c and 6b,c, the traces have been recorded both in air and under nitrogen, in order to assess the presence of oxidation processes. As expected, the total weight loss in air is larger, due to combustion of the organic anion. In this case, three defined steps can be envisaged, although the first one can be resolved into two. This can be also seen in the DTA profile. The first endothermic peak is observed below the temperature corresponding to the first endothermic peak of sample MGALCO₃, while the small endothermic effect at ca. 250 °C almost coincides with it. This means that most of the water molecules are more easily removed from the interlayer space from sample MGALT1 than from sample MGALCO₃, probably due to the hydrophobic character of the terephthalate anion. The influence of the terephthalate anion on the properties of the interlayer water was seen above in the FT-IR, where the band due to $\nu(\text{OH})$ mode was rather broad, indicating a wide distribution of hydrogen bonds with differing strengths.

From the first weight loss (18.6%) for MGALT1 recorded in air, a value of 1.06 can be calculated for the number of water molecules existing in the compound. The second weight loss may be ascribed to elimination of water through condensation of hydroxyl groups from the layers; this would represent a weight loss of 17.5% (experimental 18.3%). The total weight loss determined experimentally up to 740 °C is 57.7%, while that expected from the chemical composition, and allowing for the loss of the terephthalate anion, is 54.8%.

Traces for MGALCO₃ and MGALT1 (in air) are qualitatively similar up to ca. 500 °C; while the original hydrotalcite shows no significant weight loss above this temperature, the additional weight loss should be due to combustion of the organic anion. The slightly lower weight loss recorded in this temperature range when the analysis is performed in nitrogen should be due to decomposition of terephthalate and formation of coke on the sample surface. This is confirmed by the color of the residue after the DTA: it was white for samples MGALCO₃ and MGALCAL550 (in air) but black in the case of sample MGALCAL550 in nitrogen. Specially different are the DTA profiles for MGALT1 under air or nitrogen, Figure 6b,c. While below ca. 500 °C they are fairly similar, a sharp, very intense exothermic peak is recorded at ca. 550 °C in air, indicating the combustion of the organic anion mentioned above. The low-temperature region is more complex than for sample MGALCO₃ probably due to the existence of selective interactions between the terephthalate anion and water molecules in the interlayer. The existence of a small endothermic peak at about 254 °C may indicate some formation of carbonate during synthesis. This carbonate component may not be detected by IR (being hidden by the terephthalate group absorption) or below the accuracy of the chemical analysis. It indicates, however, the sensitivity of DTA to the charge-balancing anions.

Finally, traces for sample MGALV1 in air are shown in Figure 5d and 6d. Due to the high nuclearity of the polyoxovanadate anion, which is not removed albeit decomposed during thermal decomposition, the total weight loss is lower than for the carbonate and terephthalate-containing samples. Nevertheless, two steps are recorded in TG, the first one up to ca. 200 °C (10.9%), which represents elimination of 0.8 water molecules, and the second weight loss extending over a wide temperature range but completed by approximately 650 °C. Total weight loss was in this case 24.6% (expected 24.5%). No weight loss is associated with the vanadate. Similarly, the DTA profile shows a sharp, endothermic peak at 190 °C, due to water elimination, and a broad feature, with minima at 330 and 470 °C which most likely correspond to elimination of hydroxyl groups.

Surface Area and Porosity. In agreement with data in the literature,⁸ the TG results given above indicate that upon calcination at ≈ 200 °C the interlayer water molecules have been removed, but no indication about further weight loss originated by collapsing of the layered structure (via dehydroxylation) is observed; the weight loss up to ≈ 200 °C is associated with weight loss of interlamellar water and is comparable to that found in the organic derivatives. Calcination below this temperature, however, would give rise to samples possessing different degrees of hydration. Twu and Dutta⁸ have reported that calcination between 160–350 °C of MgAl-layered double hydroxide intercalated with decavanadate species leads to destruction of the oxometalate and the formation of cyclic and chainlike metavanadates. In our case, the FT-IR spectrum of sample MGALV2 calcined at 200 °C shows only a shoulder close to 975 cm⁻¹ in addition to stronger bands at 761 and 667 cm⁻¹, indicative of the destruction of the decavanadate structure.

Full nitrogen adsorption isotherms at -196 °C were obtained for specific surface area (SSA) and porosity assessment. Samples were degassed for 2 h at 200 °C under a residual pressure of 10⁻⁵ Torr. Specific surface areas were also determined by the single-point method,²⁶ upon degassing the samples at 200 °C for 2 h in a nitrogen stream. The specific surface areas for samples containing terephthalate were determined only using the single-point method. For other samples, values calculated using both methods were coincident within experimental error.

The nitrogen adsorption isotherms at -196 °C correspond to type II in the IUPAC classification,³⁷ although a hysteresis loop is recorded for relative pressures of 0.5–0.7, the shape of which

(37) Sing, K. S. W.; Everett, D. H.; Haul, R. A. W.; Moscou, L.; Pierotti, R.; Rouquerol, J.; Siemianowska, T. *Pure Appl. Chem.* **1985**, *57*, 603.

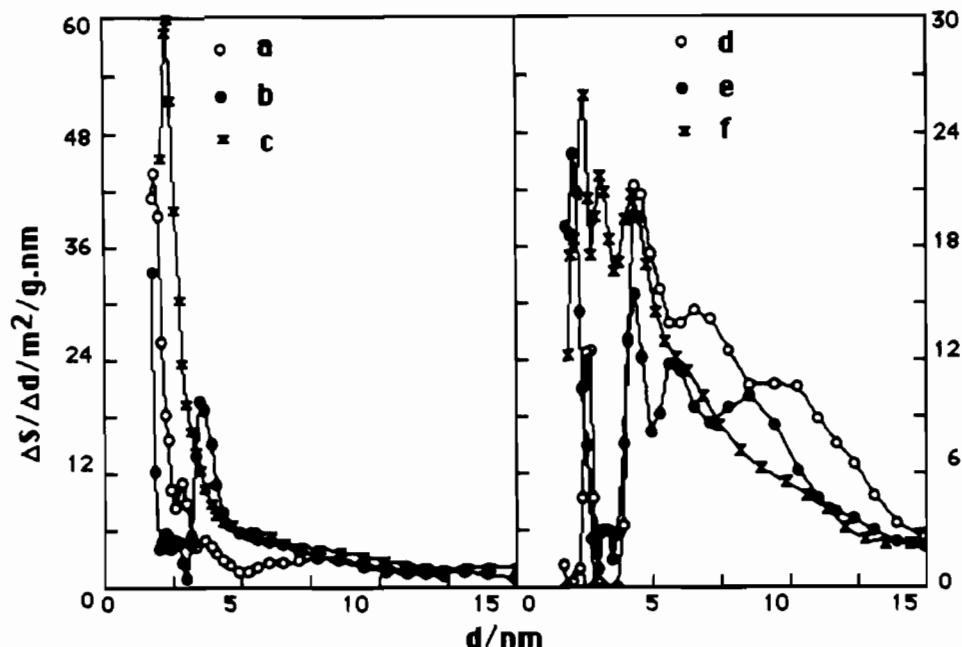


Figure 7. Pore size distribution curves for samples (a) MGALV1, (b) MGALV2, (c) MGALV2G, (d) MGALV3, (e) MGALV4, and (f) MGALV4G.

indicates the presence of pores open at both ends. This is to be expected for the morphology of the particles. BET analysis results in plots with excellent regression coefficients ($r^2 > 0.999$), yielding the values summarized in Table 2. The value determined for the original hydrotalcite, sample MGALCO3 ($77 \text{ m}^2/\text{g}$), is within the range usually reported for these such samples, although it depends markedly on sample pretreatment. It is also very sensitive to the temperature and time of crystallization and on any hydrothermal treatment given to the sample and may vary between 22 and $115 \text{ m}^2/\text{g}$.^{28,36,38,39}

Sample MGALV1 shows a reduced SSA than that observed for MGALCO3, although incorporation of vanadate to yield sample MGALV1 results in an increase up to $56 \text{ m}^2/\text{g}$. The significantly low values for samples MGALV2 and MGALV2G are rather unexpected, as PXRD data indicate that their structures correspond to a layered material.

For other samples containing vanadium the SSA values are larger than for sample MGALV1 and fairly close to that of sample MGALCO3, except for sample MGALV3 which again shows a peculiar behavior. This result would suggest that little difference exists among all these samples. The relatively low value of the surface area (when compared to zeolite or pillared clay) and the equivalence of the surface areas of the carbonate and vanadate intercalated LDHs, as well as the type II nature of the nitrogen adsorption isotherms, indicate the lack of intragallery microporosity in these materials.

Pore size distribution curves are given in Figure 7. As can be seen from this figure, the materials display either of two different characteristics. The first, for samples MGALV1, MGALV2, and MGALV2G, corresponds to a sharp distribution of pores with diameter close to 2–4 nm. For samples MGALV3, MGALV4, and MGALV4G a broad distribution is observed, with additional pores with a diameter of 6 and 10 nm, making a noticeable contribution to the specific surface area. As a result, it may be concluded the use of terephthalate is likely to favor a narrow pore size distribution through a decrease in the acid–base reaction between the POM and the LDH (or its calcined

material). If such a reaction takes place extensively during synthesis, formation of microcrystallites, undetectable by PXRD, would account for formation of interparticle pores, in addition to intraparticle, narrow pores.

Concluding Remarks

It is clear from the results presented here that a variety of methods are available which yield polyvanadate-pillared hydroxides. In so far as PXRD provides information concerning the gallery height, direct synthesis, anion exchange, and rehydration all result in similar expansion of the lattice. The use of an organic intermediate (i.e., terephthalate or glycerol) does not appear to substantially modify the nature of the powder pattern. In a similar way, FT-IR does not suggest any significant variation among the different routes. In terms of surface area and porosity, however, the choice of preparative route seems particularly important. Much sharper pore size distributions result from samples prepared via a terephthalate intermediate. Such a variation will clearly be important in catalyst preparation. At the present moment, the origin of the rather broad peak in PXRD is unclear, although the possibility of a separate aluminum-absent phase is possible. Studies are in progress in order to elucidate the nature of the polyoxometalate species formed along decomposition of these materials.

Overall, this study provides the first detailed study of inorganic pillared LDHs prepared by a variety of procedures, and it demonstrates that swelling with glycerol is not restricted to the hydroxide form of the LDH.

Acknowledgment. The authors acknowledge financial support from the CICYT (Grant MAT91-767) and the Cambridge Commonwealth Trust. This work was performed within the framework of a Joint Research grant (Accion Integrada) sponsored by the British Council (U.K.) and Ministerio de Educacion y Ciencia (Spain), reference HB85A/1991, and the Concerted European Action on Pillared Layered Solids (CEA-PLS). M.-A.U. also acknowledges financial support from Universidad de Córdoba.

(38) Martin Labajos, F. M.Sc. Thesis, University of Salamanca, Spain, 1990.
 (39) Trujillano, R. M.Sc. Thesis, University of Salamanca, Spain, 1992.